

Simultaneous observations of solar transition region blinkers and explosive events by SUMER, CDS and BBSO

Are blinkers, explosive events and spicules the same phenomenon?

M. S. Madjarska and J. G. Doyle

Armagh Observatory, College Hill, Armagh BT61 9DG, N. Ireland

Received 16 September 2002 / Accepted 11 March 2003

Abstract. The SoHO discovery of the new “blinker” phenomena focused our study on the search of its relation to already known phenomena such as explosive events and spicules. The study was performed using a specially planned joint observing program involving the Coronal Diagnostic Spectrometer (CDS), Solar Ultraviolet Measurements of Emitted Radiation spectrograph (SUMER) and Big Bear Solar Observatory (BBSO) magnetograph. Within each blinker, the SUMER data reveal the presence of small-scale ($3''$ – $5''$), short-lived (2–3 min) bright features not seen in the CDS data which has sometimes being interpreted as oscillations in SUMER data. With this data we have clearly identified UV explosive events in CDS data. The explosive events show a size close to the small-scale brightenings forming the blinker core. However, they appear in the SUMER data with their typical strong blue and red wings while the blinker shows at best only a small increase in the emission of the blue and red wings and in most instances the typical transition region red-shift in the center of the line. In all cases the explosive events cover one pixel in CDS corresponding to a size of $4'' \times 4''$ – $6''$. All identified explosive events were located at the border of the bright network i.e. the blinker, in the network or even in the internetwork. From this data, we believe that blinkers and explosive events are two separate phenomena not directly related or triggering each other. In this study, the Doppler shift was derived in a blinker phenomenon for the first time. It ranges from -5 to 25 km s^{-1} and is predominantly red-shifted. The observed magnetic flux increase during the blinker phenomena seems to play a crucial role in the development of this event. We suggest that “blinkers” maybe the on-disk signature of spicules.

Key words. Sun: corona – Sun: transition region – Sun: activity: Sun: UV radiation

1. Introduction

A new transient phenomenon named as “blinker” was first introduced and analysed by Harrison (1997) and Harrison et al. (1999) using data obtained with the Coronal Diagnostic Spectrometer (CDS) on-board SoHO. Blinkers represent an enhancement in the flux of transition region lines such as O III 599 Å, O IV 554 Å and O V 629 Å with formation temperatures 1×10^5 , 1.6×10^5 and 2.5×10^5 K, respectively. The above authors found no significant presence in lines such as Mg IX 368 Å (1×10^6 K) and Mg X 624 Å (1×10^6 K) formed at coronal temperatures. Furthermore, they found only a modest increase in the chromospheric/low transition region He I 584 Å line. However, as was already pointed out by Harrison et al. (1999), the blinker presence at ‘cool’ temperatures is still not clear, because of the optical thickness of the He I line (Brooks et al. 1999).

It was found that blinkers have a typical size of $\sim 8'' \times 8''$ and an average lifetime of ~ 16 min. The large number of longer-duration blinkers put the average blinker duration at almost 40 min (Harrison et al. 1999). Brković et al. (2001), however, using observations which permitted a better detection of shorter and longer lived brightenings, determined a lifetime in the range of 3–110 min, with an average duration of 23 min in He I, 16 min in O V and 12 min in Mg IX. The average intensity enhancement found by Harrison et al. (1999) in O V and O IV was 1.48 and 1.43, respectively. The intensity increase was 1.04 for Mg IX and 1.08 for He I, while Brković et al. (2001) found higher values of 1.09 and 1.22, respectively, which could be due to the different method of threshold determination.

Blinkers are preferentially located in the network lanes (Harrison et al. 1999; Bewsher et al. 2002). Brković et al. (2001), however, reported an appearance of brightenings also in the internetwork. Blinkers were also studied in detail both in the quiet Sun and active regions by Bewsher et al. (2002) and Parnell et al. (2002). Their analysis of the magnetic fragments in the “quiet” Sun using Michelson Doppler Imager (MDI)

Send offprint requests to: M. S. Madjarska,
e-mail: madj@star.arm.ac.uk

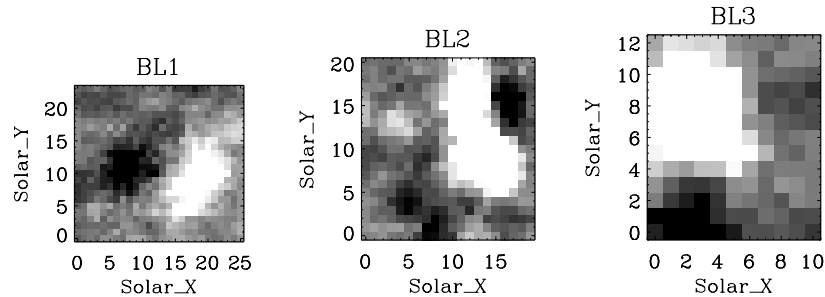


Fig. 1. Partial frame of BBSO magnetograms of the three blinker examples. The images are obtained by averaging over 15 min and are scaled from -15 to 15 Gauss. The units in Y and X axes are “arcsec”.

data showed that blinkers preferentially occur above regions of large or strong magnetic fragments with 75% occurring in regions where one polarity dominates. Priest et al. (2002) suggested five different physical mechanisms which could explain the blinker appearance: a heating of cool spicular material, a containment of plasma in low-lying loops in the network, a thermal linking of cool and hot plasma in response to a coronal heating event, and a cooling and draining of hot coronal plasma when coronal heating is switched off. They suggested that, in each case, a blinker could be produced by the granular compression of a network junction.

It is here also important to mention a study by Gallagher et al. (1999) on transient events in the transition region (using the $O\text{ V } 629\text{ \AA}$ line) and the upper chromosphere/lower transition region (using the $He\text{ I } 584\text{ \AA}$ line) registered by CDS. They observed numerous transient brightenings in network features with duration between 80 and 200 s and dimensions of 6000 and 10 000 km. Their wavelet analysis revealed a tendency for a semi-periodic behaviour, with excess power at a frequency of about 4 mHz. They derived relative line-of-sight velocities of 13 km s^{-1} with some events having velocities up to $\sim 20\text{ km s}^{-1}$ measured relative to the average quiet Sun. The main characteristics of these features are quite close to the feature called blinker but their duration does not match any of the so far observed CDS blinkers. They were interpreted by Banerjee et al. (2001) as network oscillations.

Another ultraviolet phenomenon of interest in the present study are explosive events, analysed in detail already for two decades using observations obtained by the Naval Research Laboratory High Resolution Telescope and Spectrometer (HRTS) and the Solar Ultraviolet Measurements of Emitted Radiation (SUMER) spectrograph. They are characterized by non-Gaussian profiles, have a lifetime of ~ 200 s and size $\sim 4''\text{--}5''$, showing Doppler velocities up to $\sim 200\text{ km s}^{-1}$. They are predominantly blue-shifted and are located at the boundaries of the super-granulation cells. Explosive events were found at the edges of unipolar magnetic field regions or in the magnetic network lanes characterized by a weak mixed polarity magnetic field (Dere et al. 1991; Porter & Dere 1991). The intensity ratio of $O\text{ IV } 1401.16\text{ \AA}$ and 1404.81 \AA showed a clear variation, corresponding to enhancements in the electron density by a factor of ~ 3 (Teriaca et al. 2001). The main characteristics of the explosive events were studied by Brueckner & Bartoe (1983), Dere et al. (1989), Porter & Dere (1991), Innes et al. (1997, 2001), Chae et al. (1998), Pérez et al. (1999),

Teriaca et al. (2001), Madjarska & Doyle (2002) and Teriaca et al. (2002).

A debate has started as to why explosive events are not seen in CDS data and whether the two transient events, blinkers and explosive events, are the same phenomenon. The different spectral and spatial capabilities of both spectrographs as well as the different way the observations were made, make it difficult to answer this question without simultaneous observations. Chae et al. (2000) were the first who identified blinker phenomena in SUMER observations, showing that the events consist of short-lived, small-scale brightenings which last about 2–3 min and have a size of about $3''\text{--}5''$.

It is highly likely that many of the transient features are closely related or even represent the same phenomena but given different names depending on their characteristics as observed at a particular wavelength or by a particular instrument. This paper describes observations (Sect. 2) specially performed to register simultaneously both transient phenomena in the two spectrographs SUMER and CDS, to reveal their fine structure, velocity field and appearance in relation to the network organization (Sect. 3). We also describe the temporal evolution of the underlying photospheric magnetic field associated with the blinker phenomena.

2. Observational material

In October 2001 a coordinated observing program was carried out specially to explore some of the problems related to transient phenomena in the solar atmosphere. One of the tasks of this program was to register simultaneously blinkers and explosive events in both spectrographs SUMER and CDS, paying special attention to the spatial and temporal co-alignment of both instruments. High resolution longitudinal magnetic field observations were also made in order to determine the magnetic properties of both phenomena.

2.1. SUMER

The SUMER (for details see Wilhelm et al. 1995; 1997; Lemaire et al. 1997) data were obtained on October 23, 2001 pointing the instrument on the “quiet Sun” at heliographic coordinates $X = 170''$ and $Y = 0''$. A $1'' \times 120''$ slit was used on the bottom part of detector A. The observations started at 15:26 UT and finished at 19:38 UT. No compensation for solar rotation was applied and thus for the rate of the rotation at these

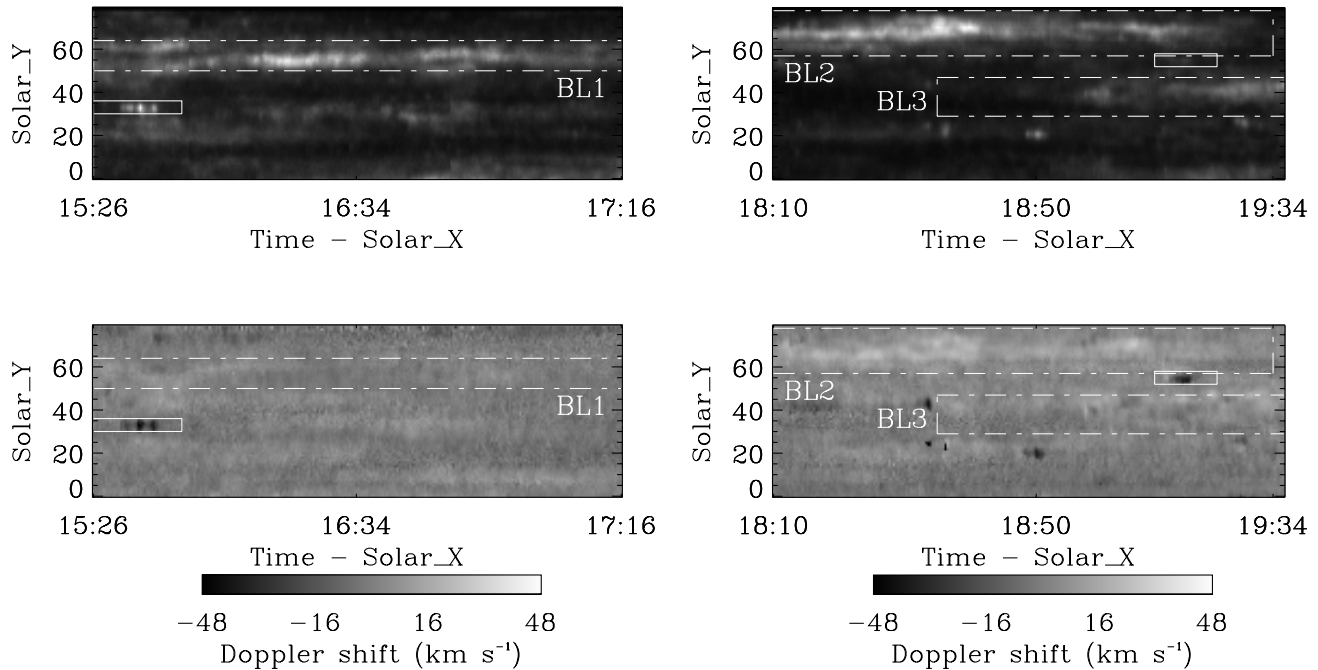


Fig. 2. *Upper panels:* three blinker events as seen in the N v 1238.82 Å intensity images, obtained by integrating over the spectral line width with the background included. *Bottom panels:* doppler shift images obtained by automatic fitting a single Gaussian. The areas indicated with ‘BL’ and dashed dotted lines represent the analysed blinker event region. The explosive events are clearly identified as the short-duration/large blue-shift features (i.e. the dark features in the plot). The units in the Y axes are “arcsec”.

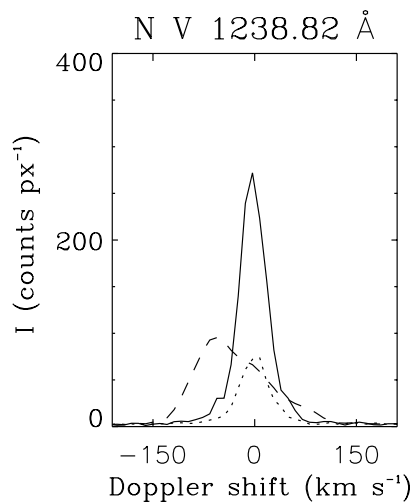


Fig. 3. The SUMER N v 1238 Å line profiles shown in a blinker brightening (solid line), during an explosive event (dashed line) and in the network (dotted line).

heliographic coordinates, the slit covered a new region of the Sun after about 400 s. A temporal sequence consisting of two spectral windows (120spatial \times 50 spectral pixels) centered on N v 1238.82 Å (2×10^5 K) and Mg IX 624.94 Å (1×10^6 K) using an exposure time of 20 s was transmitted to the ground. A full (1024 spectral \times 120 spatial pixels) reference spectrum was obtained before each temporal series. We used slit 3 which is obscured by one third by a baffle behind it (Wilhelm et al. 1995). Therefore, only 80 pixels along the slit were analysed.

The reduction of SUMER raw images involved a local gain correction, a flat-field subtraction and a correction for geometrical distortion. The signal to noise level was determined by the photon statistics.

The wavelength calibration for SUMER, which has no calibration source on-board, is usually done using chromospheric lines of neutral atoms. The C I 1245.94 Å, C I 1244.51 Å and C I 1245.53 Å lines were the only reliable reference lines found in the full spectrum. The C I lines are optically thin lines and have a formation temperature of 1.3×10^4 K. At this temperature one should account for a certain Doppler shift, e.g. Chae et al. (1998) found a red-shift for these lines of 1.5 km s^{-1} . The wavelengths of these lines are taken from Curdt et al. (2001).

2.2. CDS

CDS (Harrison et al. 1995) observations were taken in such a way that the SUMER slit remains in the CDS field-of-view during the entire observing period. The spectrometer rastered a region of the “quiet” Sun using a $4'' \times 240''$ slit with 15 s exposure time during 6 exposures. This resulted in a scanned solar region of $24'' \times 176''$. The solar_X angular pixel size was $4''.06$ and the solar_Y $1''.68$. Therefore, the resulting cadence was ~ 2 min, which corresponds to 6 SUMER exposures. The observations were made in 3 lines; O III 599.6 Å, O v 629.73 Å and Mg IX 368.07 Å. No compensation for the solar rotation was applied in order to follow the SUMER instrument.

The standard CDS procedures were applied to correct for missing pixels, CCD readout bias, cosmic rays, flat field effects and a radiometric calibration.

2.3. BBSO

The magnetograms used in the present study were obtained with the Big Bear Solar Observatory's Digital Vector Magnetograph (Spirock et al. 2001). Longitudinal magnetograms measuring the line-of-sight magnetic fields (Stokes- I' and $-V'$) of a selected region of $337'' \times 332''$ were taken every 20 s from 15:16 UT to 19:32 UT on October 23, 2001. The data were obtained by the BBSO team and provided to us after a flat-field correction had been applied. The data were also converted from an Earth to a SoHO view and a comparison was made with a few MDI high resolution images available on this day to ensure the correct co-alignment between ground based and SoHO observations. In order to follow the temporal evolution of a selected region the data needed correction for a pointing shift. Three blinkers were identified in the data (see Sect. 3.1.1), each associated with bipolar magnetic fragments (see Fig. 1).

3. Data analysis

3.1. Blinkers

3.1.1. Identification

In this work we used only two lines, CDS O v 629 Å (2.5×10^5 K) and SUMER N v 1238 Å (2×10^5 K). These two lines have similar formation temperatures which is important when comparing observations from different instruments. We also have to mention that we did not use the same line in both instruments (O v 629 Å) because this observing campaign had also another aim which required the simultaneous registration of N v 1238 Å and Mg x 625 Å by SUMER (see Teriaca et al. 2002 for details).

The identification of each blinker was performed through a visual inspection of the CDS data as was previously done by Harrison et al. (1999). The main criteria was to select features which are close to the mean blinker characteristics in size, duration and intensity enhancement. Any other brightenings with smaller size and duration were excluded. Later these features were also studied, but after a profile examination of their SUMER counterpart (see later in the paper). After the identification in the CDS data a visual co-alignment of CDS and SUMER observations was made. The SUMER solar_X angular pixel size was ~ 1 arcsec, while the CDS solar_X pixel size was 4.06 arcsec. Despite the four times different resolution we were able to find the exact CDS blinker counterpart in the SUMER data. Figure 2 shows the identification of three blinkers in N v 1238 Å whose intensity variation is discussed below.

3.1.2. Intensity variations

The result of the successful identification of the blinker phenomena in both spectrograph observations can be seen by comparing the time series in (a), (b), (c) and (d) in Figs. 4–6. At the beginning of the time series, the SUMER slit was crossing the center of a CDS blinker (Fig. 4) making it the best of the three examples. Its SUMER counterpart as seen in Fig. 4d reveals

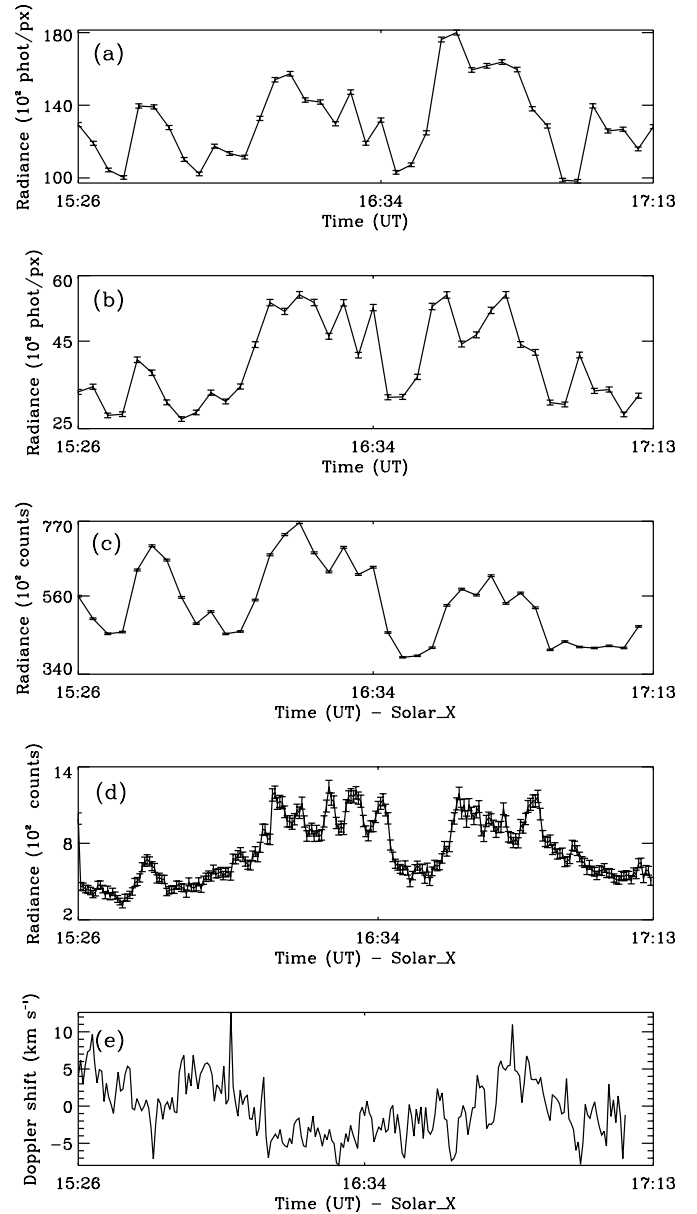


Fig. 4. **a)** CDS O v 629 Å radiance profile of blinker BL1 obtained by integrating over the blinker area. **b)** CDS O v 629 Å radiance profile in a single solar_X pixel in which the SUMER slit was centered. **c)** SUMER N v 1238 Å radiance profile after binning over 6 spectra in order to obtain the CDS cadence. **d)** SUMER radiance profile in a single pixel from the blinker area. **e)** Doppler shift profile in the same pixel as **d)** using N v 1238 Å.

the presence of several small-scale (solar_Y $\sim 3''$ – $5''$), short-lived (~ 150 s) bright features in the blinker center (they are also seen on the intensity image of Fig. 2, BL1). We show in Fig. 3 typical line profiles in a blinker brightening (solid line), an explosive event (dashed line) and a network. The blinker in Fig. 5, unfortunately, is not well covered by the SUMER slit, but nevertheless the blinker in the SUMER data can be distinguished as well as the presence of small-scale, short-lived brightenings in the blinker core (see also BL2 in Fig. 2). In the third case, the blinker has just appeared in the CDS field-of-view and again SUMER caught only the border of the blinker.

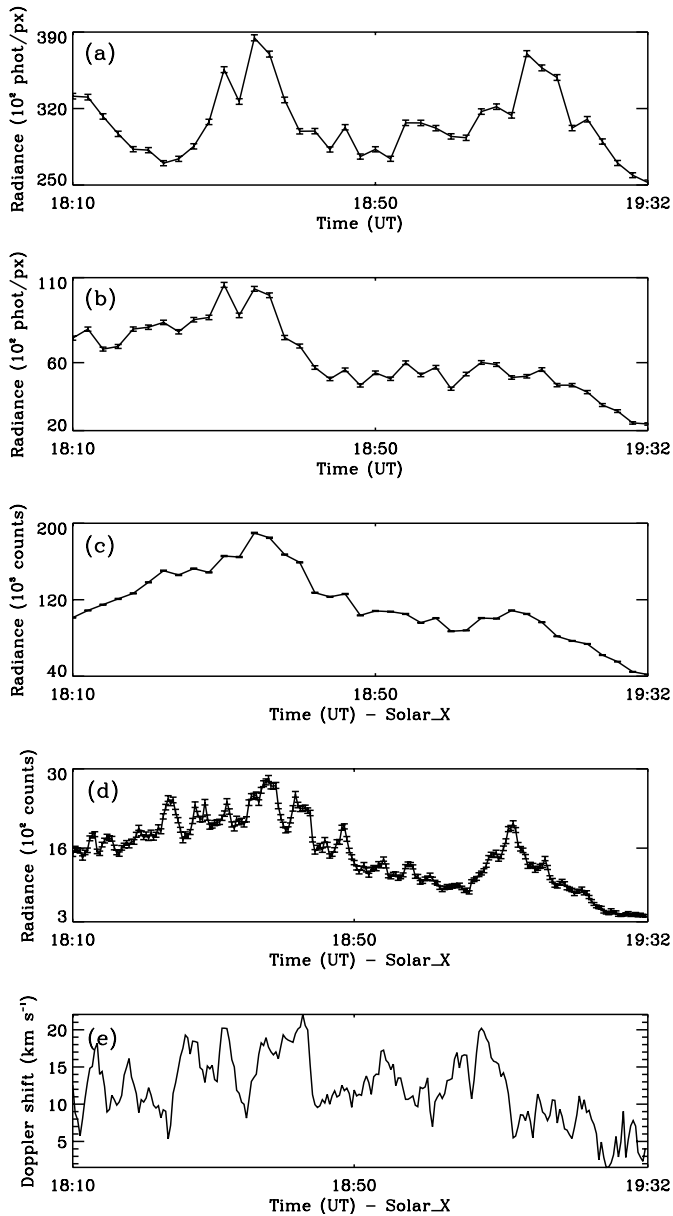


Fig. 5. **a)** CDS O v 629 Å radiance profile of blinker BL2 obtained by integrating over the blinker area. **b)** CDS O v 629 Å radiance profile in a single solar_X pixel in which the SUMER slit was centered. **c)** SUMER N v 1238 Å radiance profile after binning over 6 spectra in order to obtain the CDS cadence. **d)** SUMER radiance profile in a single pixel from the blinker area. **e)** Doppler shift profile in the same pixel as **d)** using N v 1238 Å.

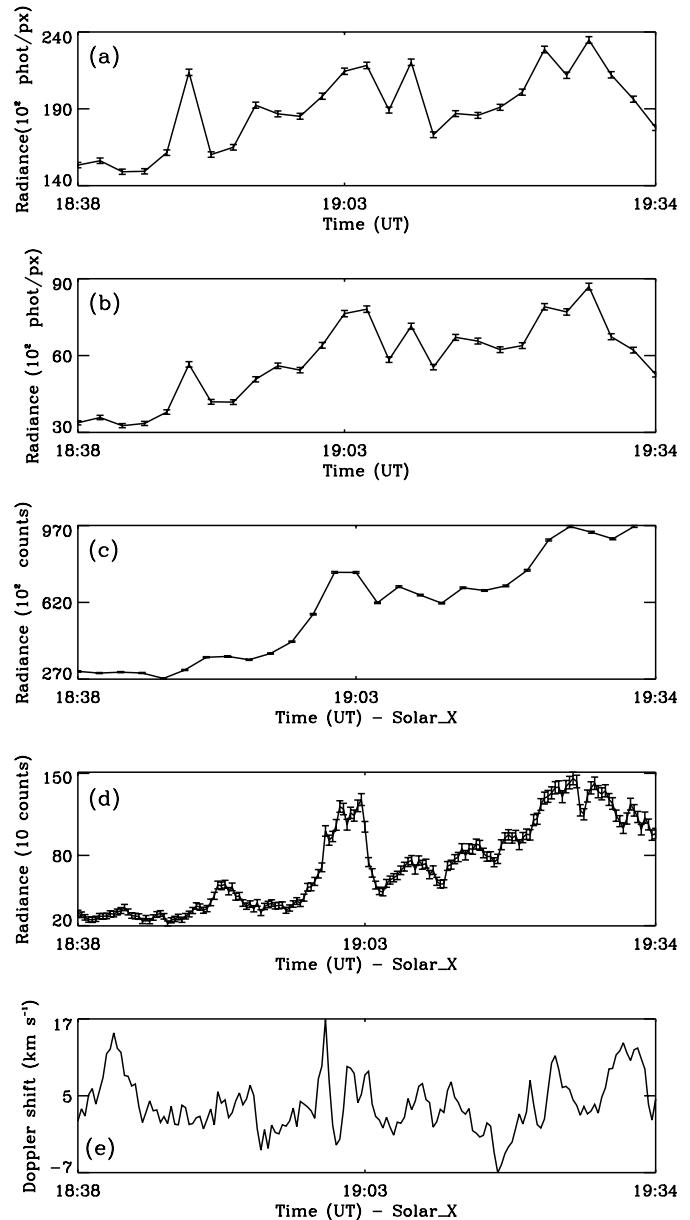


Fig. 6. **a)** CDS O v 629 Å radiance profile of blinker BL3 obtained by integrating over the blinker area. **b)** CDS O v 629 Å radiance profile in a single solar_X pixel in which the SUMER slit was centered. **c)** SUMER N v 1238 Å radiance profile after binning over 6 spectra in order to obtain the CDS cadence. **d)** SUMER radiance profile in a single pixel from the blinker area. **e)** Doppler shift profile in the same pixel as **d)** using N v 1238 Å.

Nevertheless, the feature is still present as can be seen from plot (d) in Fig. 6. Similar small-scale/short-duration brightenings are also seen in bright points (Doyle et al. 1998; Madjarska et al. 2003).

Figures 4–6a presents the temporal evolution of the integrated intensity over each blinker area as seen in the CDS O v line without the background being subtracted. Note that in some instances part of the brightening region is not in the CDS field-of-view which explains the moderate increase in intensity in these events. Figures 4–6b give the intensity profile in a CDS single solar_X pixel in which the SUMER slit was

centered. The SUMER intensity profile is shown in Figs. 4–6c. The profile is obtained by binning over 10'' along the slit which corresponds to the blinker area as identified in the CDS data and over 6 spectra in order to reduce the SUMER exposure of 20 s to the CDS 2 min cadence. These profiles (b, c) clearly show the correspondence between the blinkers identified by SUMER and CDS. Figures 4–6d display the intensity profile with the background included in a single SUMER pixel centered in the blinker area as identified in the SUMER data.

Most of the studied blinkers so far appear in the CDS data as a single, very bright pixel surrounded by a few fainter

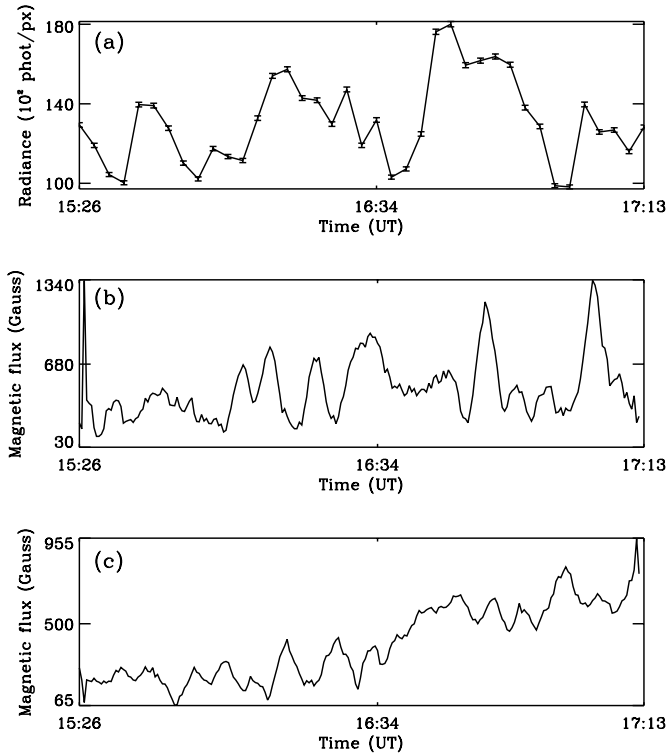


Fig. 7. **a)** CDS O v 629 Å radiance profile of blinker BL1 obtained integrating over the blinker area. **b)** The total magnetic flux from positive polarities fragments above 40 Gauss. **c)** The total magnetic flux from negative polarities fragments above 25 Gauss.

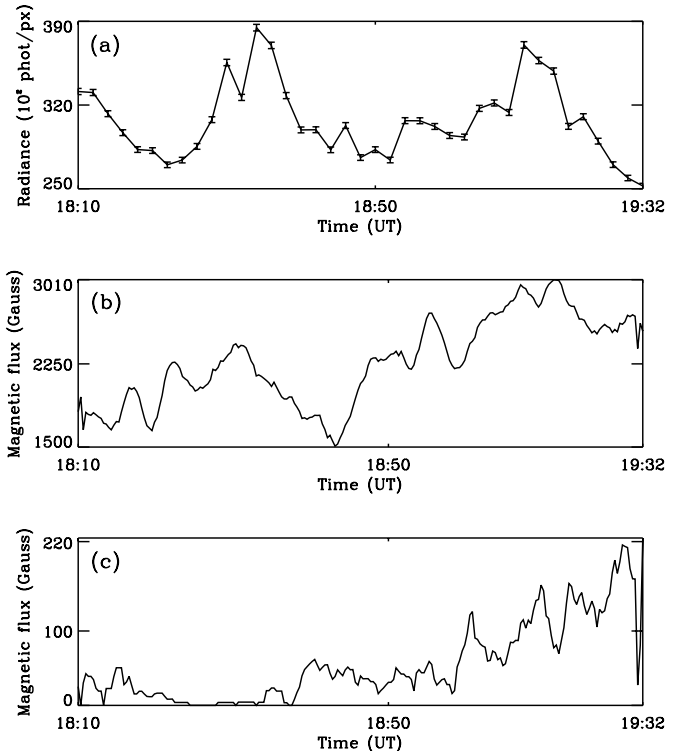


Fig. 8. **a)** CDS O v 629 Å radiance profile of blinker BL2 obtained by integrating over the blinker area. **b)** The total magnetic flux from positive polarities fragments above 40 Gauss. **c)** The total magnetic flux from negative polarities fragments above 25 Gauss.

ones. The higher resolution of SUMER data revealed the small-scale structure of the observed blinkers (see Fig. 2, upper, left panel). The SUMER blinker core consists of small-scale ($3''$ – $5''$) brightenings with a mean duration of ~ 150 s. As was mentioned before, the SUMER slit with a $1''$ size covers a new region of the Sun after ~ 400 s due to the solar rotation. Therefore, any intensity changes in a period of time of more than ~ 1200 s which corresponds to a slit moving through a ~ 3 arcsec wide feature should be accepted as temporal intensity variations in a single phenomenon of this size. We assume that the solar_X size of the brightenings is the same as their solar_Y. Therefore, the moving slit position due to the solar rotation does not affect our analysis and the subsequent conclusions. The small-scale brightenings do not always appear on the same position and can be seen a few arcsec up and down along the slit, but always remaining in the same area defined as a CDS blinker (Fig. 2).

3.1.3. Doppler shift

Apart from the identification of the observed features, more important results can be derived from an analysis of the SUMER line profiles. The N v 1238 Å is a strong line and clear from any blends. It was also registered on the KBr central part of the SUMER detector which has ~ 10 times higher detector quantum efficiency compared to the bare parts of the detectors. The wavelength calibration was performed as explained in Sect. 2.1. Figures 4–6e show the Doppler shift profile in a single SUMER pixel in which the intensity variations are

displayed in Figs. 4–6d. In the case of BL1 (Fig. 4e), the first intensity enhancement is predominantly blue-shifted (we prefer to call a blinker an event appearing at the same position and showing several intensity enhancements), while the second changes several times from blue to red-shift. The shifts appear in the range from -5 to 5 km s $^{-1}$. During BL2 (Fig. 5e) the intensity as well as the Doppler shift variations are not so well expressed, because the SUMER slit was at the blinker periphery. Nevertheless, the emission from this blinker appears to be only red-shifted in the range from 10 to 24 km s $^{-1}$ showing some temporal variations. The third example (Fig. 6e) was not well positioned in the SUMER field-of-view, but the first intensity increase is clearly visible as well as an interesting transition from a red to blue-shift and back, ranging from -5 to 17 km s $^{-1}$.

3.1.4. Magnetic flux variations

The use of the Big Bear Digital Vector Magnetograph was strongly motivated by the high resolution of the instrument. Despite the pointing shift corrections (Sect. 2.3), some slight image shift of 1–2 arcsec still remained. Thus the magnetic flux profile was obtained by selecting a rectangular area which contains the magnetic field features corresponding to the blinker (Fig. 1). The selected area was chosen 1–2 arcsec wider and higher to take into account the possibility that the pointing shift can move the feature out of the selected field-of-view. A visual analysis of a movie of the studied area was made paying

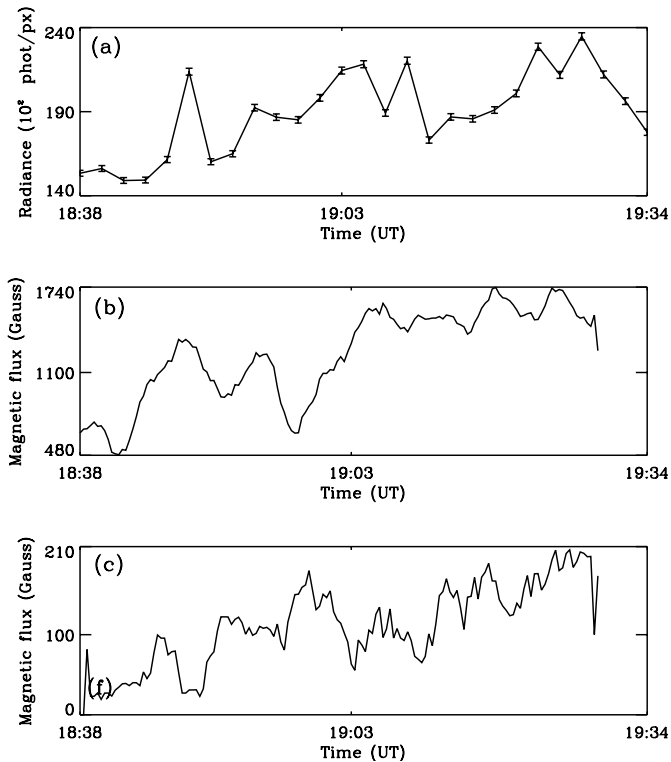


Fig. 9. **a)** CDS O v 629 Å radiance profile of blinker BL3 obtained by integrating over the blinker area. **b)** The total magnetic flux from positive polarity fragments above 40 Gauss. **c)** The total magnetic flux from negative polarity fragments above 25 Gauss.

attention that the magnetic feature remained all the time in the selected field-of-view. A co-alignment of CDS and BBSO data was done using as a reference available MDI images.

Figures 7–9a repeat the plots from Figs. 4–6a of the CDS O v 629 Å integrated intensity in the blinker area for the sake of easier comparison of the blinkers and their corresponding magnetic flux profile. Figures 7–9(b, c) show the temporal evolution of the integrated magnetic flux from the positive and negative fragments with a magnetic field above 40 and 25 Gauss, respectively. In all three cases there is a predominant presence of positive flux. In BL2 and BL3, the negative flux emerges during the observations while BL1 was associated with a bipolar region which was present before the observations had started. During the first brightening of BL1 (Fig. 7), the positive flux increases about 4 times showing temporal changes with a duration ~ 150 s. The negative polarity flux also shows some increase, but it does not seem to play an important role in the blinker appearance. The second brightening of BL1 has only one short strong increase in the positive flux, but at the same time the negative flux shows a significant rise. The last strong positive flux increase is related to the last brightening which is not covered by the SUMER slit.

BL2 in Fig. 8 shows a positive flux increase only by a factor of ~ 1.5 during the first brightening. The temporal changes are difficult to distinguish, but some flux fluctuations are definitely present. The negative flux is very low and probably does not play a significant role. During the second brightening, the positive flux shows a more significant increase of ~ 2 times,

and is accompanied by a stronger temporally changing negative flux.

The third blinker example (Fig. 9) is more difficult to analyse. In fact, it only partially appeared in the SUMER and CDS field-of-view (see Sect. 3.1.2). We enlarged the BBSO field-of-view by another 3 arcsec in order to get the entire magnetic fragment which corresponds to this blinker. In this case the magnetic field increase does not show the fluctuation pattern as visible in BL1 but the increase of the magnetic flux is still present, reaching a value of about 2.6 times the pre-event one. The negative polarity features show a stronger contribution than in BL2.

3.2. Explosive events

For a long time, the lack of explosive events identification in CDS data was a quite puzzling question. Such an identification could explain the relation or the difference between explosive events and blinkers. The present observations permitted the two features to be identified simultaneously in both instruments. First, the explosive events were selected in the SUMER data after visual inspection of the line profiles. The explosive events can easily be identified in the Doppler shift maps of Fig. 2 as the features with the highest Doppler shift. Since the blue wing of explosive events is usually the predominant one, the automatic single Gaussian fitting produced a fit towards the blue, but in many cases a red wing was also present. After a precise co-alignment the events were also found in the CDS data. In all cases the explosive events cover one pixel in CDS solar_X (remember that the angular pixel size is $4''.06$) and 2–3 pixels in solar_Y direction corresponds to a size of $4'' \times 4''$ – $6''$, the typical size of these phenomena.

All identified explosive events are located at the border of the bright network i.e. the blinker (Chae et al. 2000), in the network or even in the internetwork space. However, because of the CDS resolution they look much closer to the blinker or even seem to be part of this phenomenon. From the SUMER data it is clear that this is not the case (Fig. 2).

Figures 11–12 show the results for two of the observed explosive events seen in Fig. 2. Figures 11–12a give the intensity profile in the CDS explosive event area while Figs. 11–12b is their counterpart in the SUMER data. The SUMER intensity profile was obtained after binning along the slit over the explosive event area and over 6 spectra in order to rescale the SUMER exposure of 20 s to the CDS 2 min cadence. The correspondence between the two profiles is clear in both examples. Figures 11–12c present the intensity profile in the explosive event without binning and Figs. 11–12d the Doppler shift profile obtained via automatic single Gaussian fitting. Since the data were obtained during the SoHO post-recovery period (2001), the CDS instrumental width is already quite large. Therefore only the SUMER line profiles during explosive events showing very large wings will appear in the CDS data as features with an enlarged width and a blue-shifted line center (Fig. 10). In any other case only a brightening in a few CDS pixels will be registered. Thus, an explosive event

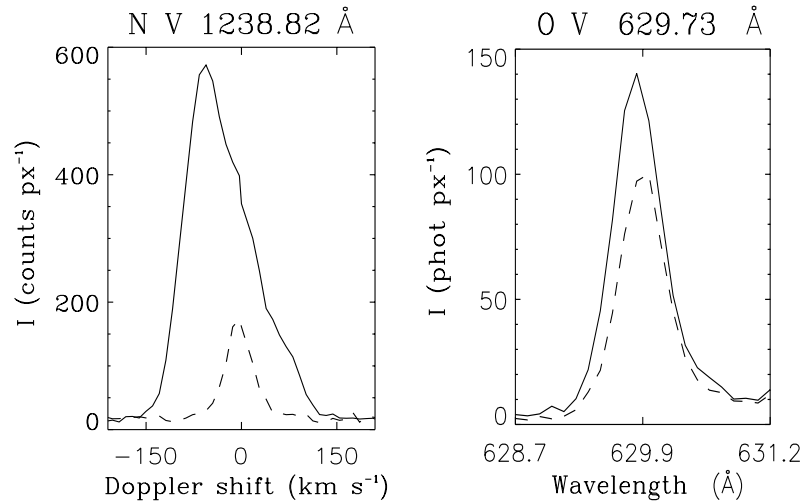


Fig. 10. *Left panel:* the SUMER N v 1238 Å line profile during (solid line) and after (dashed line) an explosive event. The profile is obtained by binning over 6 pixels along the slit. *Right panel:* the CDS O v 629 Å line profile during (solid line) and after (dashed line) the explosive event shown in the left panel as identified in the SUMER data. The profiles are obtained by binning over 3 pixel in Solar_Y direction.

identification in CDS data without having their SUMER equivalent would be a difficult task.

The integrated intensity increase during the explosive events appears to be a factor of ~ 2 , and in some cases even higher. Therefore they will appear in the CDS data as a simple brightening event, which looks like a typical intensity increase during a blinker. Therefore, it is very possible that many of the short time lived blinkers and those appearing in the internetwork space found by Brković et al. (2001) were in fact explosive events.

3.3. Are blinkers and explosive events the same phenomenon?

The discovery of the blinker features opened a discussion on whether blinkers and explosive events are the same phenomenon. Blinker phenomena were first identified in CDS observations, while the explosive events were only found in SUMER data. Chae et al. (2000) first identified the features in the two instruments concluding that blinkers and explosive events look different because of their different size, duration and location. The authors claimed, however, that blinkers consist of “many small-scale and short-lived SUMER unit brightening events having a size and duration that is comparable to those of explosive events”. The authors suggested that the difference in spectral characteristics between unit brightening events and explosive events might be attributed to the different magnetic reconnection geometries.

With our study we made an attempt to give observational evidences for the appearance of both events in the two spectrometers using a specially designed observing program. Several observed explosive events show a size close to the small-scale brightenings forming the blinker core. However, they appear in the SUMER data with their typical strong blue and red wings while blinkers show at best only a small increase in the emission of the blue and red wings (e.g. see Fig. 3) with in most instances the typical transition region red-shift in the

center of the line (e.g. see Figs. 5 and 6). The explosive events appear at different positions in the network border or even in the internetwork. Often blinkers appear with no explosive event close-by. They show predominantly red-shifted emission (up to 25 km s^{-1}), while the explosive events are in most cases predominantly blue-shifted ($\sim 150 \text{ km s}^{-1}$). Blinkers were associated with bipolar magnetic regions, showing an increase of the magnetic flux during the brightening, but neither magnetic cancellation was detected nor a particular temporal variation of the total magnetic flux. We were not able to associate explosive events with any particular magnetic field pattern.

The blinkers and explosive events main characteristics described above make us believe that they are more likely two separate phenomena not directly related or triggering each other.

4. Discussion and conclusions

We studied in detail the appearance and main characteristics of blinkers and explosive events during simultaneous SUMER, CDS and BBSO observations. The blinker phenomena were clearly identified in the SUMER data and their fine structure was resolved. As has already being concluded by Chae et al. (2000), a blinker consists of several small-scale brightenings of $3''$ – $5''$ size and duration of ~ 2 – 3 min. In this study the Doppler shift was derived in a blinker phenomenon for the first time. It ranges from -5 to 25 km s^{-1} and is predominantly red-shifted. A transition from blue to red-shifted emission in the course of the 200 – 300 s observations was also detected. The magnetic flux changes of both opposite polarities during the blinker phenomena seems to play a crucial role in the development of this event.

Gallagher et al. (1999) found pulse-like transient brightenings of $8''$ – $15''$ in size in the quiet Sun network and a duration of 200 s. They were correlated with locations of red-shifted line emission in CDS O v and He I. The authors suggested that these brightenings are produced via rapid compression of the

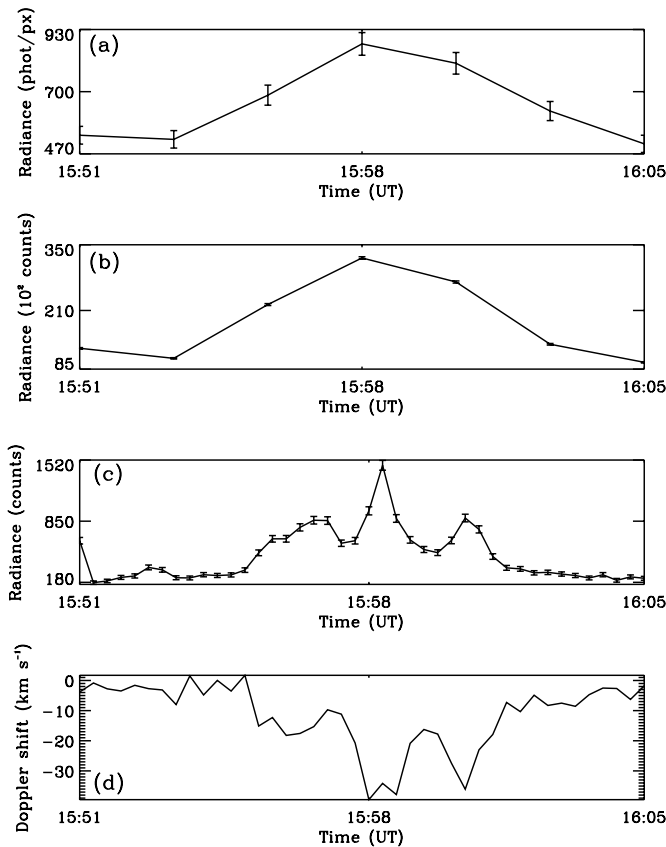


Fig. 11. **a)** CDS O v 629 Å radiance profile obtained by integrating over the explosive event area. **b)** SUMER N v 1238 Å radiance profile after binning over 6 spectra in order to obtain the CDS cadence. **c)** SUMER radiance profile in a single pixel from the explosive event without binning. **d)** Doppler shift profile in the same pixel as **c)**. An automatic single Gaussian fit has been performed to obtain the Doppler shift shown in this figure. Since the blue wing of explosive events is usually the predominant one, such a fitting will produce a Gaussian profile towards the blue. We show in the left panel of Fig. 10 the N v 1238 Å line profile during this explosive event (solid line).

transient region plasma assuming that the intensity of the optically thin O v line is quadratically proportional to the local electron density. These features strongly resemble the small-scale brightenings identified in the present study which suggests that they probably belong to blinker events as well. The only difference comes from the different sizes, but that could be simply explained with the different resolution of SUMER and CDS.

The blinker appearance in SUMER observations raise the question whether the SUMER bright network is not in fact a so called CDS blinker. Our analysis of the observations presented here show that any bright SUMER network is associated with a CDS blinker. A forthcoming study on the bright network using similar data sets will try to confirm this result. At the same time the analysis of most of the shorter lived brightenings in the CDS data and their counterpart in SUMER show that they appear to be explosive events.

Blinker characteristics obtained in this paper support the suggestion by Priest et al. (2002) of a possible association of blinkers with an ejection of cool chromospheric plasma – solar

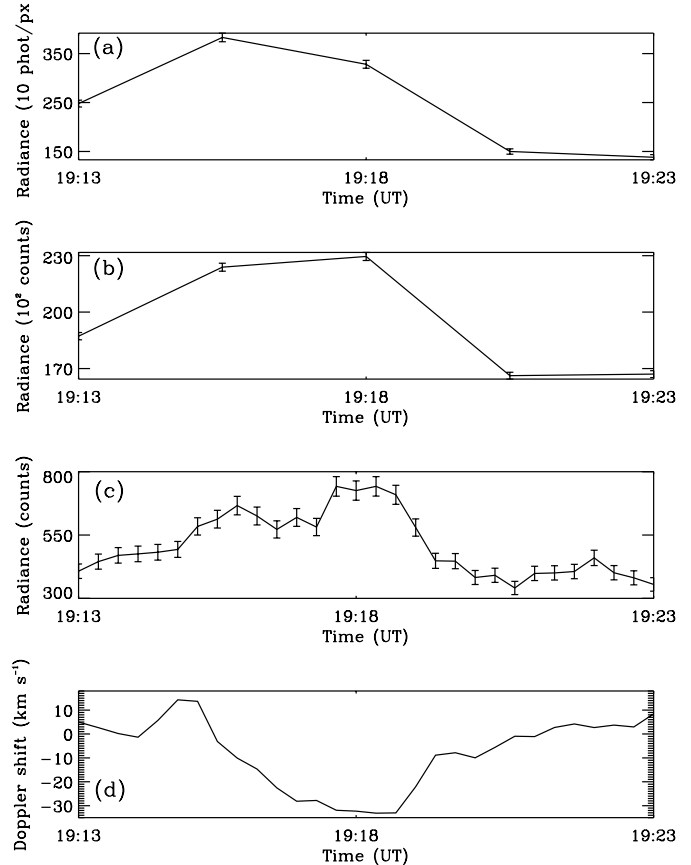


Fig. 12. **a)** CDS O v 629 Å radiance profile obtained by integrating over the explosive event area. **b)** SUMER N v 1238 Å radiance profile after binning over 6 spectra in order to obtain the CDS cadence. **c)** SUMER radiance profile in a single pixel from the explosive event without binning. **d)** Doppler shift profile in the same pixel as **c)**.

spicules (see a recent review by Wilhelm 2000 and the references therein). The physical characteristics of the small-scale brightenings forming a blinker core, their Doppler shifts and size, together with their location in the network strongly support this idea. The unique SUMER observations of solar spicules and macro-spicules presented by Wilhelm (2000) showed the presence of spicules everywhere in the network in spectral lines such as O v and N v. We show in Fig. 13 a raster in the SUMER O v 629 Å and N v 1238 Å lines taken close to the limb on 31 August 1996 which clearly show many spicule-like features appearing on-disk as a bright network. The N v 1238 Å image is quite similar although parts of the image look more smeared which could be related to the fact that lines from Li-like ions have a long tail in their ionization fraction extending to higher temperatures and are known to have 2–5 higher emission measure than lines formed at similar temperatures, suggested to be due to a density dependence in the ionization balance (Vernazza & Raymond 1979).

Wilhelm (2000) derived spicule Doppler shifts of ± 30 km s⁻¹ relative to the mean spectral position of the O v 629 Å line and macro-spicules having line-of-sight velocities (in N v) of up to 150 km s⁻¹ suggesting that macro-spicules are most likely associated with explosive events. Zachariadis et al. (2001), using Sacramento Peak H α observations, found that bright limb spicules have their origin in bright

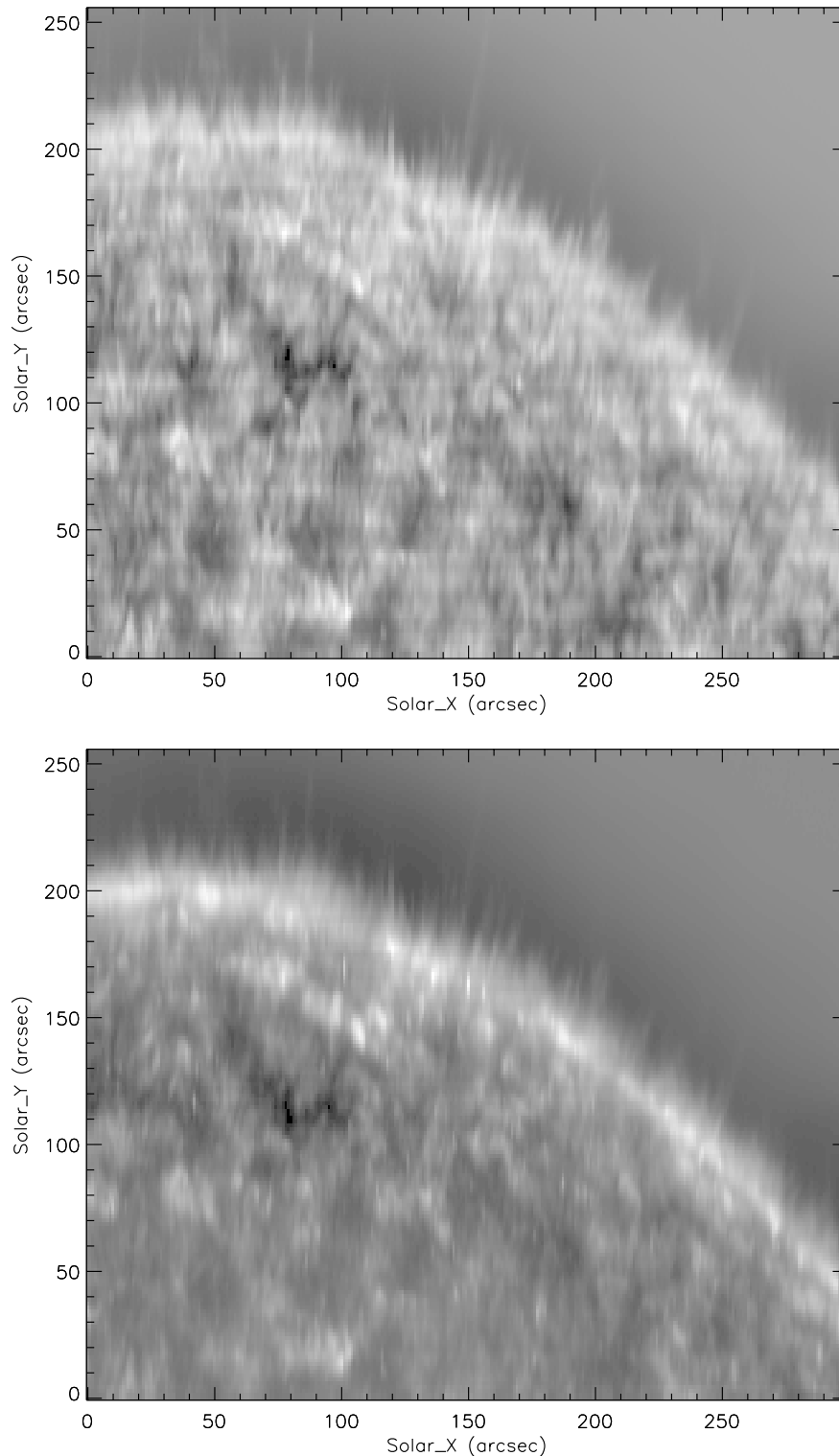


Fig. 13. Intensity images in O V 629 Å (upper panel) and N V 1238 Å (bottom panel) obtained on 31 August 1996. The scan covers a polar region showing the network and numerous spicules (Wilhelm 2000).

mottles on the disk. Therefore, we have to expect that spicules should be seen in any SUMER disk observation in spectral lines covering the temperature range in which solar spicules could be registered. Peter (2001), in an analysis of Gaussian fits to mid-transition region lines, identified two components. A narrow core component which showed the familiar transition region

red-shifts and a broader component which he associated with coronal funnels. Although the wings in the blinker line profile are small in the 20 s exposure spectra examined here, it is conceivable that they would become somewhat larger in longer exposure profiles covering larger areas, as examined by e.g. Peter (2001). Hence it is possible that spicules are the source of the

broad components of the transition region lines, observed on the Sun (Peter 2001) and on other stars (Wood et al. 1997).

Acknowledgements. We want to thank J. Varsik for help with the BBSO image processing and to BBSO for the observing time. Research at Armagh Observatory is grant-aided by the N. Ireland Dept. of Culture, Arts and Leisure. This work was supported by PPARC grant PPA/GIS/1999/00055. The SUMER project is financially supported by DLR, CNES, NASA, and PRODEX. We would also like to thank the CDS and SUMER teams, in particular A. Fludra and P. Lemaire for their help in planning these observations.

References

- Banerjee, D., O'Shea, E., Doyle, J. G., & Goosens, M. 2001, *A&A*, 371, 1137
- Bewsher, D., Parnell, C. E., & Harrison, R. A. 2002, *Sol. Phys.*, 206, 21
- Brooks, D. H., Fischbacher, G. A., Fludra, A., et al. 1999, *A&A*, 347, 277
- Brković, A., Solanki, S. K., & Rüedi, I. 2001, *A&A*, 373, 1056
- Brueckner, G. E., & Bartoe, J.-D. F. 1983, *ApJ*, 272, 329
- Chae, J., Wang, H., Lee, C. Y., Goode, P. R., & Schühle, U. 1998, *ApJ*, 497, L109
- Chae, J., Haimin, W., & Goode, Ph. 2000, *ApJ*, 528, 119
- Curdt, W., Brekke, P., Feldman, U., et al. 2001, *A&A*, 375, 591
- Dere, K. P., Bartoe, J.-D. F., & Brueckner, G. E. 1989, *Sol. Phys.*, 123, 41
- Dere, K., Bartoe, J.-D. F., Brueckner, G. E., Ewing, J., & Lund, P. 1991, *J. Geophys. Res.*, 96, 9399
- Doyle, J. G., van den Oord, G. H. J., O'Shea, E., & Banerjee, D. 1998, *Sol. Phys.*, 181, 51
- Gallagher, P. T., Phillips, K. J. H., Harra-Murnion, L. K., Baudin, F., & Keenan, F. P. 1999, *A&A*, 348, 251
- Harrison, R. A., Sawyer, E. C., Carter, M. K. et al. 1995, *Sol. Phys.*, 162, 233
- Harrison, R. A. 1997, *Sol. Phys.*, 175, 467
- Harrison, R. A., Lang, J., Brooks, D. H., & Innes, D. E. 1999, *A&A*, 351, 1115
- Innes, D. E., Inhester, B., Axford, W. I., & Wilhelm, K. 1997, *Nature*, 386, 811
- Innes, D. E. 2001, *A&A*, 378, 1067
- Lemaire, P., Wilhelm, K., Curdt, W., et al. 1997, *Sol. Phys.*, 170, 105
- Madjarska, M. S., & Doyle, J. G. 2002, *A&A*, 382, 319
- Madjarska, M. S., Teriaca, L., Doyle, J. G., & Banerjee, D. 2003, *A&A*, 398, 775
- Parnell, C. E., Bewsher, D., & Harrison, R. A., 2002, *Sol. Phys.*, 206, 249
- Pérez, M. E., Doyle, J. G., Erdélyi, R., & Sarro, L. M. 1999, *A&A*, 342, 279
- Peter, H. 2001, *A&A*, 374, 1108
- Porter, J. G., & Dere, K. P. 1991, *ApJ*, 379, 775
- Priest, E. R., Hood, A. W., & Bewsher, D. 2002, *Sol. Phys.*, 205, 249
- Spirock, T., Denker, C., Chen, H., et al. 2001, *ASP Conf. Proc.*, 236, 65
- Teriaca, L., Madjarska, M. S., & Doyle, J. G. 2001, *Sol. Phys.*, 200, 91
- Teriaca, L., Madjarska, M. S., & Doyle, J. G. 2002, *A&A*, 392, 309
- Vernazza, J. E., & Raymond, J. C. 1979, *ApJ*, 228, L89
- Wilhelm, K., Curdt, W., Marsch, et al. 1995, *Sol. Phys.*, 162, 189
- Wilhelm, K., Lemaire, P., Curdt, W., et al. 1997, *Sol. Phys.*, 170, 75
- Wilhelm, K. 2000, *A&A*, 360, 351
- Wood, B. E., Linsky, J. L., & Ayres, T. R. 1997, *ApJ*, 478, 745
- Zachariadis, Th. G., Dara, H. C., Alissandrakis, C. E., Koutchmy, S., & Gontikakis, C. 2001, *Sol. Phys.*, 202, 41